Numerical Homogenization of Heterogeneous Anisotropic Linear Elastic Materials

S. Margenov, S. Stoykov, Y. Vutov

Institute of Information and Communication Technologies,
Bulgarian Academy of Sciences

Abstract. The numerical homogenization of anisotropic linear elastic materials with strongly heterogeneous microstructure is studied. The developed algorithm is applied to the case of trabecular bone tissue. In our previous work [1], the orthotropic case was considered. The homogenized anisotropic tensor is transformed according to the principle directions of anisotropy (PDA). This provides opportunities for better interpretation of the results as well as for classification of the material properties.
The upscaling procedure is described in terms of six auxiliary elastic problems for the reference volume element (RVE). Rotated trilinear Rannacher-Turek finite elements are used for discretization of the involved subproblems. A parallel PCG method is implemented for efficient solution of the arising large-scale systems with sparse, symmetric, and positive semidefinite matrices. Then, the bulk modulus tensor is computed from the upscaled stiffness tensor and its eigenvectors are used to define the transformation matrix. The stiffness tensor of the material is transformed with respect to the PDA which gives a canonical (unique) representation of the material properties.
Numerical experiments for two different RVEs from the trabecular part of human bones are presented.

1 Introduction

Many materials, including the human bone have a complex microstructure. In recent years micro computed tomography (μCT) and micro finite element method (μFEM) analysis proved to be a valuable tool for analyzing bone properties, see e.g. [2]. The macro level material properties strongly depend on their microstructure. Nevertheless, the overall mechanical responses can be described using multilevel techniques that are built upon basic conservation principles at the micro level.

In our previous work [1], we studied a numerical homogenization algorithm for computing the upscaled orthotropic stiffness tensor. This approach is further developed to the general case of anisotropic materials. Here we obtain an effective stiffness tensors of a reference volume element (RVE).

The trabecular bone is a strongly heterogeneous composition of solid and fluid phases. Its voxel representation obtained from μCT images is used to formulate the problem. Our goal is to obtain upscaled material properties of trabecular

bone tissue. In this work, only the mechanical response of the solid phase is considered. To this purpose a fictitious domain approach is used.

This paper is organized as follows. The applied numerical homogenization scheme is described in Section 2. In Section 3 transformation to the principal directions of anisotropy (PDA) is recalled. And finally the upscaled and transformed tensors are presented and discussed in the last section.

2 Homogenization Technique

Let Ω be a parallelepipedal domain representing our reference volume element (RVE) and $\mathbf{u} = (u_1, u_2, u_3)$ be the displacements vector in Ω. Here, components of the small strain tensor [3] are:

$$\varepsilon_{ij}\left(\mathbf{u}\left(\mathbf{x}\right)\right) = \frac{1}{2}\left(\frac{\partial u_i(\mathbf{x})}{\partial x_j} + \frac{\partial u_j(\mathbf{x})}{\partial x_i}\right) \tag{1}$$

We assume that Hooke's law holds. The stress tensor σ is expressed in the form

$$\sigma_{ij} = s_{ijkl}\varepsilon_{kl}, \tag{2}$$

where summation over repeating indexes is assumed. The forth-order tensor s is called the stiffness tensor, and has the following symmetry [4]:

$$s_{ijkl} = s_{jikl} = s_{ijlk} = s_{klij}. \tag{3}$$

Often, the Hooke's law is written in matrix form:

$$\begin{bmatrix}\sigma_{11}\\ \sigma_{22}\\ \sigma_{33}\\ \sigma_{23}\\ \sigma_{13}\\ \sigma_{12}\end{bmatrix} = \begin{bmatrix} s_{1111} & s_{1122} & s_{1133} & s_{1123} & s_{1113} & s_{1112}\\ s_{2211} & s_{2222} & s_{2233} & s_{2223} & s_{2213} & s_{2212}\\ s_{3311} & s_{3322} & s_{3333} & s_{3323} & s_{3313} & s_{3312}\\ s_{2311} & s_{2322} & s_{2333} & s_{2323} & s_{2313} & s_{2312}\\ s_{1311} & s_{1322} & s_{1333} & s_{1323} & s_{1313} & s_{1312}\\ s_{1211} & s_{1222} & s_{1233} & s_{1223} & s_{1213} & s_{1212}\end{bmatrix} \begin{bmatrix}\varepsilon_{11}\\ \varepsilon_{22}\\ \varepsilon_{33}\\ 2\varepsilon_{23}\\ 2\varepsilon_{13}\\ 2\varepsilon_{12}\end{bmatrix}. \tag{4}$$

The symmetric 6×6 matrix in (4) is denoted with S and. is called also the stiffness matrix. For an isotropic material matrix S, and the tensor s have only two independent degrees of freedom. For orthotropic materials (materials containing three orthogonal planes of symmetry), the matrix S has nine independent degrees of freedom. In the general anisotropic case, S has 21 independent degrees of freedom [5].

The goal of our study is to obtain homogenized material properties of the trabecular bone tissue. In other words – to find the stiffness tensor of a homogeneous material which would have the same macro-level properties as our RVE. Our approach follows the numerical upscaling method from [1] (see also [6, 7]). The homogenization scheme requires finding Ω-periodic functions $\xi^{kl} = (\xi_1^{kl}, \xi_2^{kl}, \xi_3^{kl})$, k, $l = 1, 2, 3$, satisfying the following equation in a week formulation:

$$\int_\Omega \left(s_{ijpq}(x)\frac{\partial \xi_p^{kl}}{\partial x_q}\right)\frac{\partial \phi_i}{\partial x_j}d\Omega = \int_\Omega s_{ijkl}(x)\frac{\partial \phi_i}{\partial x_j}d\Omega, \tag{5}$$

for an arbitrary Ω-periodic variational function $\phi \in H^1(\Omega)$. After computing the characteristic displacements ξ^{kl}, from (5) we can compute the homogenized elasticity tensor s^H using the following formula:

$$s^H_{ijkl} = \frac{1}{|\Omega|} \int_\Omega \left(s_{ijkl}(x) - s_{ijpq}(x) \frac{\partial \xi^{kl}_p}{\partial x_q} \right) d\Omega. \tag{6}$$

From (5) and due to the symmetry of the stiffness tensor (3), we have the relation $\xi^{kl} = \xi^{lk}$. Therefore the solution of only six problems (5) is required to obtain the homogenized stiffness tensor.

The periodicity of the solution implies the use of periodic boundary conditions. Rotated trilinear (Rannacher-Turek) finite elements [8] are used for the numerical solution of (5). This choice is motivated by the additional stability of the nonconforming finite element discretization in the case of strongly heterogeneous materials [9]. Construction of a robust non-conforming finite element method is generally based on application of mixed formulation leading to a saddle-point system. By the choice of non continuous finite elements for the dual (pressure) variable, it can be eliminated at the (macro)element level. As a result we obtain a symmetric positive semi-definite finite element system in primal (displacements) variables. We utilize this approach, which is referred as the *reduced and selective integration* (RSI) [10].

For the solution of the arising linear system, the preconditioned conjugate gradient is used. For the construction of the preconditioner the isotropic variant of the displacement decomposition (DD)[11] was used. We write the DD auxiliary matrix in the form

$$C_{DD} = \begin{bmatrix} A & & \\ & A & \\ & & A \end{bmatrix} \tag{7}$$

where A is the stiffness matrix corresponding to the bilinear form

$$a(u^h, v^h) = \sum_{e \in \Omega^h} \int_e E \left(\sum_{i=1}^{3} \frac{\partial u^h}{\partial x_i} \frac{\partial v^h}{\partial x_i} \right) de. \tag{8}$$

Such approach is motivated by the second Korn's inequality, which holds for the RSI FEM discretization under consideration. More precisely, in the case of isotropic materials, the estimate

$$\kappa(C_{DD}^{-1} K) = O((1 - 2\nu)^{-1})$$

holds uniformly with respect to the mesh size parameter in the FEM discretization, where ν is the Poisson ratio.

As the arising linear systems are large, the problems are solved in parallel. Parallel MIC(0) preconditioner for scalar elliptic systems [12] is used to approximate (7). Its basic idea is to apply MIC(0) factorization of an approximation B of the stiffness matrix A. Matrix B has a special block structure. Its diagonal

blocks are diagonal matrices. This allows the solution of the preconditioning system to be performed in parallel. The condition number estimate $\kappa(B^{-1}A) \leq 3$ holds uniformly with respect to mesh parameter and possible coefficient jumps (see for the related analysis in [12]). This technique is applied three times – once for each diagonal block of (7). Thus we obtain the parallel MIC(0) preconditioner in the form:

$$C_{DDMIC(0)} = \begin{bmatrix} C_{MIC(0)}(B) & & \\ & C_{MIC(0)}(B) & \\ & & C_{MIC(0)}(B) \end{bmatrix}.$$

More details on applying this preconditioner for the proposed homogenization technique can be found in [1].

3 Principal Directions of Anisotropy

We follow the procedure for determining the PDA described in [13]. A coordinate system is said to coincide with the PDA of a material, when the material, subjected to "all-around uniform pure extension state," forms a "pure tension state."

Let us introduce the bulk modulus tensor

$$K = \begin{bmatrix} K_{11} & K_{12} & K_{13} \\ K_{21} & K_{22} & K_{23} \\ K_{31} & K_{32} & K_{33} \end{bmatrix}. \tag{9}$$

The elements of K are defined as

$$K_{ij} = \sum_{k=1}^{3} s_{ijkk} \tag{10}$$

We write the "all-round uniform extension" as $\varepsilon_{ij} = \tilde{\varepsilon}\delta_{ij}$, where $\tilde{\varepsilon}$ is a constant reference strain and δ_{ij} is the Kronecker delta. Then, the stress components are

$$\sigma_{ij} = K_{ij}\tilde{\varepsilon}. \tag{11}$$

Hence the principal directions of the tensor K coincide with the stress principal directions. The stress values in these principal directions are

$$\sigma_{ij} = \lambda_i \tilde{\varepsilon}\delta_{ij}, \tag{12}$$

where λ_i are the eigenvalues of the tensor K. To ensure uniqueness of the transformation, we order the eigenvalues $\lambda_3 \geq \lambda_2 \geq \lambda_1$, i.e. the biggest eigenvalue is the third and the smallest is the first. With this order, we enforce the material to orient its strongest direction in z axis and its weakest in x. The case of equal eigenvalues, leads to equivalence of the material in two or more directions. The transformation matrix T, which rotates the coordinate system to the one which

coincides with the PDA, is given by the corresponding normalized eigenvectors v^i of K:

$$T = \begin{bmatrix} v_1^1 & v_2^1 & v_3^1 \\ v_1^2 & v_2^2 & v_3^2 \\ v_1^3 & v_2^3 & v_3^3 \end{bmatrix}. \tag{13}$$

Now we are able to rotate the stress tensor using formula

$$\bar{s}_{klst} = s_{mnpr} T_{km} T_{ln} T_{sp} T_{tr}. \tag{14}$$

Here summation over repeating indexes is assumed.

4 Numerical Experiments

To solve the above described upscaling problem, a portable parallel FEM code is designed and implemented in C++. The parallelization has been facilitated using the MPI library [14].

The analyzed test specimens are parts of trabecular bone tissue extracted from a high resolution computer tomography image [15]. The voxel size is 37 μm. The trabecular bone has a strongly expressed heterogeneous microstructure composed of solid and fluid phases.

Homogenized properties of two different RVEs with sizes of $128 \times 128 \times 128$ are shown, see Fig. 1. The RVEs are different, but part of the same vertebra. The Young modulus and the Poisson ratio of the solid phase, taken from [16], are $E^s = 14.7$GPa and $\nu^s = 0.325$. Our intention is to obtain the homogenized elasticity tensor of the RVE, taking into account the elastic response of the solid phase only. We interpret the fluid phase as a fictitious domain. Thus, we set Young modulus $E^f = \zeta E^S$ for the voxels corresponding to the fluid phase. The parameter ζ is set to 10^{-5}. The choice of ζ is studied in [1]. We also set $\nu^f = \nu^s$. The chosen values of E^f and ν^f practically do not influence the homogenization result.

The iteration stopping criterion is $||\mathbf{r}^j||_{C^{-1}}/||\mathbf{r}^0||_{C^{-1}} < 10^{-6}$, where $\mathbf{r}^j$ is the residual at the j-th iteration step of the preconditioned conjugate gradient method and C stands for the used preconditioner.

Numerical experiments are performed on a Blue Gene/P machine. It is a massively parallel computer consisting of quad-core computing nodes. The PowerPC based low power processors run at 850 MHz. Each node has 2GB of RAM. The nodes are interconnected with several specialized high speed networks—3D mesh network for peer to peer communications and tree network for collective communications, among others.

The computations were performed on 256 processors. The computations took between 4 and 5 hours for each of the auxiliary problems. This has notable increase from the case where a truly periodic media is considered [1]. In that case the number of iterations (and thus the compute time) for similar problems was around six times less.

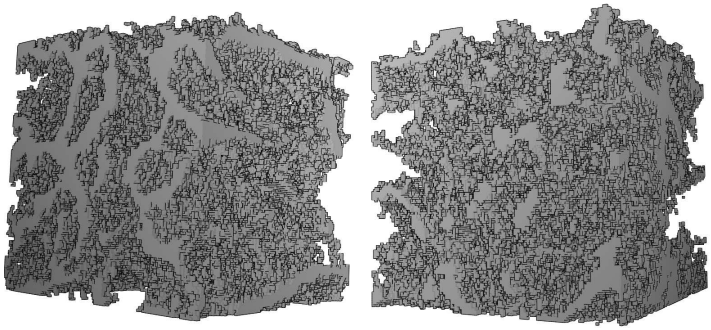

First specimen Second specimen

Fig. 1. Structure of the two RVEs.

The computed homogenized stiffness matrix for the first specimen is

$$S_1^H = \begin{bmatrix} 802 & 218 & 212 & -11.7 & -1.31 & 72.8 \\ 218 & 566 & 167 & -16.2 & 0.25 & 48.5 \\ 212 & 167 & 133 & -71.4 & 31.8 & 22.8 \\ -11.7 & -16.2 & -71.4 & 206 & 31.7 & 2.91 \\ -1.31 & 0.25 & 31.8 & 31.7 & 313 & -9.11 \\ 72.8 & 48.5 & 22.8 & 2.91 & -9.11 & 197 \end{bmatrix}, \tag{15}$$

and for the second one —

$$S_2^H = \begin{bmatrix} 372 & 127 & 74.6 & -4.75 & 4.01 & -20.0 \\ 127 & 436 & 81.3 & -9.03 & 3.60 & -16.2 \\ 74.6 & 81.3 & 606 & -44.5 & 27.8 & -11.8 \\ -4.75 & -9.03 & -44.5 & 98.2 & -21.0 & 1.68 \\ 4.01 & 3.60 & 27.8 & -21.0 & 100 & -6.17 \\ -20.0 & -16.2 & -11.8 & 1.68 & -6.17 & 120 \end{bmatrix}. \tag{16}$$

All values are measured in megapascals (MPa). The transformation procedure, described in Section 3, is applied to the stiffness matrices S_1^H and S_2^H. As a result, the stiffness matrices $\bar{S}_1^H$ and $\bar{S}_2^H$, characterizing the properties of the considered RVEs in the coordinate systems aligned with their PDA are obtained:

$$\bar{S}_1^H = \begin{bmatrix} 501 & 221 & 154 & 8.36 & -14.0 & -17.8 \\ 221 & 847 & 224 & 8.41 & -6.89 & 18.1 \\ 154 & 224 & 1340 & -16.7 & 20.9 & -0.28 \\ 8.36 & 8.41 & -16.7 & 320 & 14.2 & 9.20 \\ -14.0 & -6.89 & 20.9 & 14.2 & 196 & 1.64 \\ -17.8 & 18.1 & -0.28 & 9.20 & 1.64 & 204 \end{bmatrix}, \tag{17}$$

$$\bar{S}_2^H = \begin{bmatrix} 343 & 121 & 848 & 31.7 & 3.75 & 5.45 \\ 121 & 372 & 139 & 38.8 & -10.7 & -3.90 \\ 84.8 & 139 & 573 & -70.6 & 7.02 & -1.54 \\ 31.7 & 38.8 & -70.6 & 165 & 8.17 & -9.42 \\ 3.75 & -10.7 & 7.02 & 8.17 & 97.3 & 22.5 \\ 5.45 & -3.90 & -1.54 & -9.42 & 22.5 & 119 \end{bmatrix}. \tag{18}$$

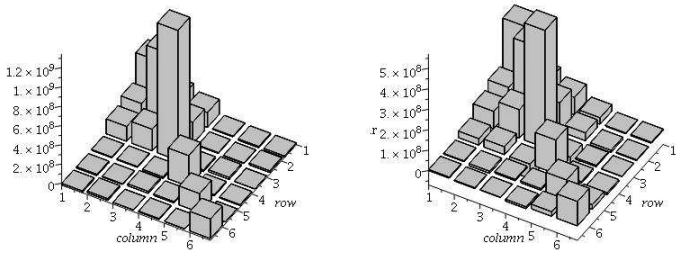

First specimen Second specimen

Fig. 2. Structure of the two transformed stiffness matrices.

The matrices $\bar{S}_1^H$ and $\bar{S}_2^H$ are visualized on Fig. 2. The degree of anisotropy η can be defined as the ratio

$$\eta = \bar{s}_{3333}/\bar{s}_{1111}. \tag{19}$$

The degrees of anisotropy for the two RVEs η_1 and η_2 are 2.67 and 1.67. One can see that although part of the same vertebra, the two specimens have different degrees of anisotropy and different magnitudes of the elastic moduli. This demonstrates the importance of the material microstructure for the elastic response.

It is well known, that the trabecular bone tissue adapts to the stresses it experiences (a fact referred to as a Wolffs law) [17]. In agreement with this, the presented homogenized stiffness tensors show considerable level of anisotropy. Our results evidently confirm that the anisotropy cant be neglected in the simulations. As a next step in this study, the analysis of a representative set of CT images is needed to provide data for correlation analysis of the homogenized stiffness tensors. Then, the map of principle directions of the experienced loads for a particular bone at the organ level will provide new opportunities for more realistic patient specific simulations using the clinically available information for the bone density.

In this context, let us remind that the presented results use very high resolution X-ray CT scans. Due to the level of radiation intensity, such a full length organ-level scanning is not applicable in-vivo. In this sense, the more standard multiscale approach is not applicable due to the lack of data.

In addition, the fluid phase of the bone plays an important part in its elastic response. One possible approximation of this two-phase system is to interpret the fluid as an almost incompressible elastic material (see, e.g., [18]). One important future goal is to verify the related results in a comparison with some more general poroelastic (say Biot) models.

Acknowledgments

This work is supported in part by Grants DFNI I01/5 and DCVP-02/1 from the Bulgarian NSF and the Bulgarian National Center for Supercomputing Applications (NCSA), giving access to the IBM Blue Gene/P computer.

The research is also partly supported by the project AComIn ,,Advanced Computing for Innovation", grant 316087, funded by the FP7 Capacity Programme (Research Potential of Convergence Regions)

References

1. S. Margenov and Y. Vutov, Parallel MIC(0) Preconditioning for Numerical Upscaling of Anisotropic Linear Elastic Materials, Large-Scale Scientific Computing, I. Lirkov, S. Margenov, J. Waniewski eds., Lecture notes in computer sciences, 5910, 2012, Springer, pp. 805-812.
2. A. J. Wirth, T. L. Mueller, W. Vereecken,C. Flaig, P. Arbenz, R. Mller, and G. H. van Lenthe, (2010). Mechanical competence of bone-implant systems can accurately be determined by image-based micro-finite element analyses. Archive of applied mechanics, 80(5), 513-525.
3. Y. C. Fung, Foundations of Solid Mechanics, Prentice-Hall, 1965.
4. A. Nayfeh, P. Pai, Linear and Nonlinear Structural Mechanics, John Wiley & Sons, 2004.
5. I. Sokolonikoff, Mathematical Theory of Elasticity, Mc-Graw-Hill, 1956.
6. R. H. W. Hoppe and S. I. Petrova, Optimal shape design in biomimetics based on homogenization and adaptivity, *Math. Comput. Simul.*, **65** (3), 2004, 257–272.
7. A. Bensoussan, J. L. Lions, and G. Papanicolaou, *Asymptotic analysis for periodic structures*, Elsevier, 1978.
8. R. Rannacher and S. Turek, Simple nonconforming quadrilateral Stokes element, *Numer. Methods for Partial Differential Equations*, **8** (2), 1992, 97–112.
9. D. N. Arnold and F. Brezzi, Mixed and nonconforming finite element methods: Implementation, postprocessing and error estimates, *RAIRO, Model. Math. Anal. Numer.*, **19**, 1985, 7–32.
10. D. Malkus, T. Hughes. Mixed finite element methods. Reduced and selective integration techniques: an uniform concepts. *CMAME* 15: 63-81, 1978.
11. R. Blaheta, Displacement decomposition–incomplete factorization preconditioning techniques for linear elasticity problems, *NLAA*, **1** (2), 1994, 107–128.
12. P. Arbenz, S. Margenov, and Y. Vutov, Parallel MIC(0) preconditioning of 3D elliptic problems discretized by Rannacher-Turek finite elements, *Computers and Mathematics with Applications*, **55** (10), 2008, 2197–2211.
13. Rand, Omri, and Vladimir Rovenski. Analytical methods in anisotropic elasticity: with symbolic computational tools. Birkhuser Boston, 2004.
14. D. Walker and J. Dongarra, MPI: a standard Message Passing Interface, *Supercomputer*, **63**, 1996, 56–68.
15. G. Beller, M. Burkhart, D. Felsenberg, W. Gowin, H.-C. Hege, B. Koller, S. Prohaska, P. I. Saparin, and J. S. Thomsen, Vertebral body data set esa29-99-l3, `http://bone3d.zib.de/data/2005/ESA29-99-L3/`.
16. S. Cowin,*Bone poroelasticity*, J. Biomechanics, **32** (1999), 217-238.
17. J. Wolff, The Law of Bone Remodeling, Berlin Heidelberg NY: Springer, 1986
18. N. Kosturski, S. Margenov: Numerical Homogenization of Bone Microstructure, Large-Scale Scientific Computations 2009, Springer LNCS 5910, pp. 140-147